

## Article

The Jurassic epiphytic macrolichen  
*Daohugouthallus* reveals the oldest lichen-plant  
interaction in a Mesozoic forest ecosystem

Qiuxia Yang,  
Yanyan Wang,  
Robert Lücking, ...,  
Hu Li, Yongjie  
Wang, Xinli Wei

tigerleecau@hotmail.com  
(H.L.)  
wangyjosmy@foxmail.com  
(Y.W.)  
weixl@im.ac.cn (X.W.)

**Highlights**

Direct fossil evidence for  
the oldest epiphytic lichen  
was provided

The earliest lichen-plant  
interaction traced back to  
165 million years ago

Energy dispersive X-ray  
spectroscopy was first  
used in lichen adpression  
fossil

Geometric morphometric  
analysis was first used to  
assess systematics of fossil  
lichen

Yang et al., iScience 26,  
105770  
January 20, 2023 © 2022 The  
Author(s).  
[https://doi.org/10.1016/  
j.isci.2022.105770](https://doi.org/10.1016/j.isci.2022.105770)

## Article

The Jurassic epiphytic macrolichen *Daohugouthallus* reveals the oldest lichen-plant interaction in a Mesozoic forest ecosystem

Qiuxia Yang,<sup>1,10</sup> Yanyan Wang,<sup>1,10</sup> Robert Lücking,<sup>2</sup> H. Thorsten Lumbsch,<sup>3</sup> Zhenyong Du,<sup>4</sup> Yunkang Chen,<sup>5,6</sup> Ming Bai,<sup>7</sup> Dong Ren,<sup>8</sup> Jiangchun Wei,<sup>1</sup> Hu Li,<sup>4,\*</sup> Yongjie Wang,<sup>9,\*</sup> and Xinli Wei<sup>1,11,\*</sup>

## SUMMARY

Lichens are well known as pioneer organisms or stress-tolerant extremophiles, potentially playing a core role in the early formation of terrestrial ecosystems. Epiphytic macrolichens are known to contribute to the water- and nutrient cycles in forest ecosystem. But due to the scarcity of fossil record, the evolutionary history of epiphytic macrolichens is poorly documented. Based on new fossil of Jurassic *Daohugouthallus ciliiferus*, we demonstrate the hitherto oldest known macrolichen inhabited a gymnosperm branch. We applied energy dispersive X-ray spectroscopy and geometric morphometric analysis to complementarily verify lichen affinity of *D. ciliiferus* and quantitatively assess the potential relationships with extant lichenized lineages, providing new approaches for study of this lichen adpression fossil. Considering the results, and the inferred age of *D. ciliiferus*, a new family, Daohugouthallaceae, is established. This work updates current knowledge to the early evolution of epiphytic macrolichens and reveals more complex lichen-plant interactions in a Jurassic forest ecosystem.

## INTRODUCTION

Lichens are a stable symbiosis composed of fungi and algae and/or cyanobacteria, also including a diverse microbiome.<sup>1,2</sup> Lichens are components of mostly terrestrial ecosystems from the polar regions to the tropics,<sup>3</sup> growing on all kinds of substrata, including bark, rock, leaf and soil.<sup>4</sup> Particularly epiphytic lichens growing on trees have been known to significantly contribute to water and nutrient cycling in forest ecosystems.<sup>5</sup> The lichen symbiosis is considered a crucial event in the evolution and transition of fungi from water to land, having evolved independently in different fungal lineages.<sup>2</sup> However, the evolutionary history of lichen-forming fungi is poorly understood, because of the sparse fossil record, and has been primarily reconstructed based on molecular dating analyses.<sup>6–9</sup> Although these approaches proposed a framework to illustrate how the lichen symbiosis may have evolved, fossil evidence is indispensable in testing and supplementing the current understandings especially when the earlier fossil was discovered.

To date, 190 fossils have been accepted to represent genuine lichens,<sup>2</sup> among which 90% are amber-preserved, and only three permineralized and charcoalfied fossils are over 100 My old.<sup>2,10,11</sup> The earliest convincing lichens are two crustose lichens from the Devonian, i.e., *Cyanolichenomycites devonicus* and *Chlorolichenomycites salopensis* (419–411 Mya), which were inferred to be saxicolous or terricolous.<sup>10</sup> Nevertheless, early evidence for foliose and fruticose lichens (so-called macrolichens) is particularly scarce. It has been proposed that the diversification of most modern macrolichens did not occur before the Cretaceous-Paleogene (K–Pg) boundary 65 Mya.<sup>6,9,12</sup> This is contrasted by the finding of the oldest Jurassic macrolichen, *Daohugouthallus ciliiferus*.<sup>13</sup> Given this lack of evidence for macrolichen fossils prior to the K–Pg boundary, the significance of the Jurassic lichen *D. ciliiferus* is crucial for understanding the evolutionary history of macrolichens.

Because macrolichens have evolved in convergent fashion in multiple, unrelated lineages in Ascomycota and Basidiomycota,<sup>8,14</sup> it is vital to clarify the systematic position of *D. ciliiferus*. Unfortunately, diagnostic features, such as hamathecium, ascus, and ascospore structure, are not known from this fossil, which renders its exact classification challenging. Therefore, it is difficult to establish relationships between fossil and extant lichens, including when taking fossils as calibration points in molecular dating analyses.<sup>2</sup> The fossil

<sup>1</sup>State Key Laboratory of Mycology, Institute of Microbiology, Chinese Academy of Sciences, Beijing 100101, China

<sup>2</sup>Botanischer Garten, Freie Universität Berlin, 14195 Berlin, Germany

<sup>3</sup>Science & Education, The Field Museum, Chicago, IL 60605, USA

<sup>4</sup>Department of Entomology, MOA Key Lab of Pest Monitoring and Green Management, College of Plant Protection, China Agricultural University, Beijing 100193, China

<sup>5</sup>School of Agriculture, Ningxia University, Yinchuan 750021, China

<sup>6</sup>College of Plant Protection, Agricultural University of Hebei, Baoding 071001, China

<sup>7</sup>Key Laboratory of Zoological Systematics and Evolution, Institute of Zoology, Chinese Academy of Sciences, Beijing 100101, China

<sup>8</sup>College of Life Sciences and Academy for Multidisciplinary Studies, Capital Normal University, Beijing 100048, China

<sup>9</sup>Guangdong Key Laboratory of Animal Conservation and Resource Utilization, Guangdong Public Laboratory of Wild Animal Conservation and Utilization, Institute of Zoology, Guangdong Academy of Sciences, Guangzhou 510260, China

<sup>10</sup>These authors contributed equally

<sup>11</sup>Lead contact

\*Correspondence: tigerleecau@hotmail.com (H.L.), wangyjosmy@foxmail.com (Y.W.), weixl@im.ac.cn (X.W.)  
<https://doi.org/10.1016/j.isci.2022.105770>



material of *D. ciliiferus* was first described as a lichen-like organism,<sup>15</sup> but more convincing evidence to support its lichen affinity was only presented a decade later.<sup>13</sup> Herein, based on new material of *D. ciliiferus*, we expand the knowledge of this hitherto oldest known macrolichen, including its photobiont relation with Jurassic gymnosperms in Mesozoic forest ecosystem. To further assess the potential significance of this fossil, we applied two new methods: (1) Energy dispersive X-ray spectroscopy (EDX), which was employed to distinguish and verify the fungal hyphae especially algal cells from the rock particles as another potential strategy of scanning electron microscopy (SEM), on the adpression fossil; and (2) geometric morphometric analysis (GMA), used to assess potential morphological relationships of *D. ciliiferus* with extant macrolichen lineages. GMA mainly uses landmarks and outlines for assessing the morphological structure of samples, transforming it into digital information,<sup>16</sup> allowing quantitative analysis of the data,<sup>17</sup> and avoiding problems stemming from subjective ad-hoc analysis of morphological characters.<sup>18</sup> GMA has become popular in the taxonomy of higher taxa including morphological variability and diversity, and even evolution of body structure.<sup>19–22</sup> In parallel, we updated the molecular clock analysis by Nelsen et al.,<sup>9</sup> which because of the comprehensive sampling offers a much broader framework than other molecular clock studies including lichen formers.<sup>7,23</sup> As a result, a new family Daohugouthallaceae is proposed to accommodate the Jurassic macrolichen which is most similar to Parmeliaceae but remains as *incertae sedis* within Ascomycota class Lecanoromycetes.

## RESULTS

### EDX analysis and the lichen nature of *D. ciliiferus*

EDX is an analytical method for analytical or chemical characterization of materials, which can give a spectrum correlated with the elemental composition of the samples<sup>24</sup>; it has been used to examine lichen mycobionts in amber-preserved lichens, indicating containing sodium, magnesium, silicon, potassium, calcium, and chlorine.<sup>25</sup> Herein, we employed EDX analysis to test whether there were the significant differences between lichen body and surrounding rock, which was treated as a potential way to determine the lichen affinity of the adpression fossil.

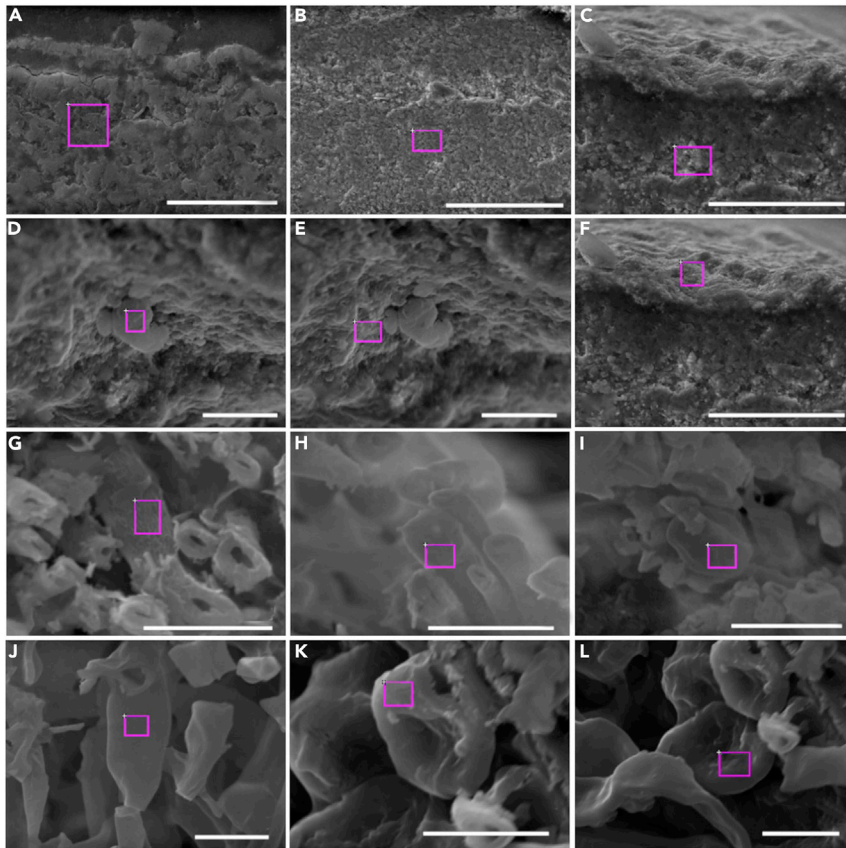
The elements and atomic percentages in the examined samples using EDX analysis (see [STAR Methods](#), [Table S1](#) and [Figure 1](#)) showed distinct differences between the fossil and rock areas, containing 100% carbon (C), and 20% carbon as well as additional elements, such as oxygen (O, more than 50%), silicon (Si, 17–22%), C (15–23%) and minor potassium (K) and aluminum (Al), respectively. The considered fungal hyphae and the adhesive photobiont cells examined from the fossil are highly consistent with the corresponding components from the extant lichens, except containing minor Si (less than 3%). Moreover, the consistency is more obvious between the fossil and the chlorolichen. Therefore, although there is no much comparability between the EDX results of amber-preserved and adpression fossils, it is feasible to distinguish the adpression lichen mycobiont and photobiont from rock by the EDX, and the photobiont seems more like extant green algae.

### GMA on the fossil and extant macrolichens

The GMA of 149 images ([Figure S1](#)) resulted in cumulative values for all the principal components, listed in [Table S2](#). The cumulative eigenvalues for the main axes (principal components) with the cumulative variance of the first four principal components amounting to 66.9% ([Table S2](#)), meeting the requirements for geometric morphometric analysis. Among the canonical variate analysis (CVA) for four combinations of the four principal components (individual variances 35.7, 14.1, 10.8, 6.3; [Figure 2](#)), the plot combining the first two principal components (cumulative variance 49.8) showed that the fossil *D. ciliiferus* (group 2) appeared morphologically closest to foliose Parmeliaceae (group 3, Lecanoromycetes, Ascomycota), including the genera *Hypotrachyna*, *Hypogymnia* and two foliose Parmeliaceae fossils.<sup>2,12</sup>

### Molecular clock assessment

The order- and family-level correspond to 176–194 Mya and 111–135 Mya in Lecanoromycetes as calculated.<sup>7</sup> We used the detailed molecular clock tree provided by Nelsen et al.<sup>9</sup> to illustrate inferred ages for selected family-level clades in the Lecanoromycetes that include macrolichens ([Figure 3](#)). Most of the families have stem node ages younger than 100 Mya, a few were reconstructed as between 150 and 100 Mya, and only one family, i.e., Lcmadophilaceae, with an inferred crown node age of approximately 200 Mya. *D. ciliiferus*, with the age of 165 My, is older than almost all the macrolichen families ([Figure S2](#)) except Lcmadophilaceae. However, members of Lcmadophilaceae differ strongly in morphology and ecology from

**Figure 1. Scanning Electron Microscopy (SEM) with Energy Dispersive X-ray Spectroscopy (EDX/EDS)**

The EDX spectra values of the examined samples seen in Table S1. The examined locations of rock and lichen fossil *Daohugouthallus ciliiferus* CNU-LICHEN-NN2020001 marked by the purple square frames are as follows from a to f.

(A) Random location 2 of rock areas.

(B) Random location 1 of rock areas.

(C) Rock under the lichen fossil.

(D) Photobiont cell of fossil lichen.

(E) Fungal hyphae of fossil lichen.

(F) Lichen fossil. The examined locations of extant chlorolichen *Hypotrachyna cirrhata* HMAS-L 8322 marked by the purple square frames are as follows from g to i.

(G) Fungal hyphae 1.

(H) Fungal hyphae 2.

(I) Green algal cell. The examined locations of extant cyanolichen *Peltigera praetextata* HMAS-L 13030 marked by the purple square frames are as follows from j to l.

(J) Fungal hyphae.

(K) Cyanobacterial cell 3.

(L) Cyanobacterial cell 1. Scale bars: a = 20  $\mu\text{m}$ ; b = 100  $\mu\text{m}$ ; c, f = 50  $\mu\text{m}$ ; d, e, h-l = 10  $\mu\text{m}$ ; g = 9  $\mu\text{m}$ .

*D. ciliiferus*, preferring terrestrial substrates such as acid soil or peat.<sup>26</sup> In addition, macrolichen genera within Lecanophilaceae distinctly diversified after the K–Pg boundary: *Siphula* approximately 48 Mya and *Thamnolia* about 16 Mya (Figures S2 and 3A). Although Umbilicariaceae, Pannariaceae, Collemataceae, and Peltigeraceae, are as old as the fossil (Figure 3A), they do not fit morphologically and/or ecologically.<sup>27–29</sup> Otherwise, Parmeliaceae is the best candidate showing the best morphological and ecological fit in GMA (Figure 2), but that family is also rejected as home for the fossil, because of its significantly younger divergence time comparing with the fossil (Figure 3A). Outside of Lecanoromycetes, other macrolichens but distinct in phenotype as presented by GMA results such as Arthoniomycetes (Ascomycota), Lichinomycetes (Ascomycota), and Agaricales (Basidiomycota), correspond to 289 Mya, 168 Mya, and 136 Mya, respectively.<sup>23</sup> If these estimates are correct, the Jurassic *D. ciliiferus* may be treated as a new clade at least in family level and reflect a new evolutionary scenario of early macrolichens.

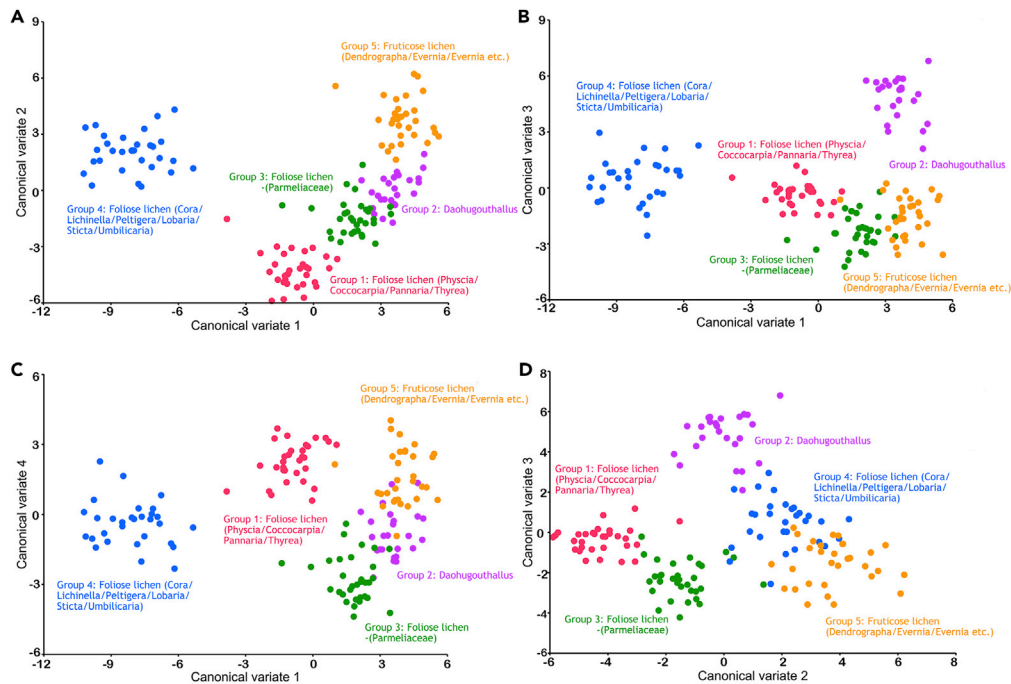


**Figure 2. CVA plots based on the geometric morphometrics analysis (the first four principal components)**

(A) CVA plot based on the highest Cumulative value 49.816 corresponding to the sum of the first principal component with the Variance value 35.713 and the second (14.104).

(B) CVA plot based on the Cumulative value 46.466 corresponding to the sum of the first principal component with the Variance value 35.713 and the third (10.753).

(C) CVA plot based on the Cumulative value 42.051 corresponding to the sum of the first principal component with the Variance value 35.713 and the fourth (6.338).

(D) CVA plot based on the Cumulative value 24.857 corresponding to the sum of the second principal component with the Variance value 14.104 and the third (10.753). Different colors represented different groups (Table S4). The distance showed the degree of similarity between different groups.

### Establishment of a new family

Based on the results from the GMA and molecular clock assessments, a new family, Daohugouthallaceae, is proposed here to accommodate *D. ciliiferus*, which has the most similarity in thallus morphology to foliose Parmeliaceae of Lecanoromycetes.

**Daohugouthallaceae** X.L. Wei, D. Ren & J.C. Wei, fam. nov. (Figure 4) —Fungal Names FN570853.

**Diagnosis:** Thallus corticolous, foliose to subfruticose, lobes irregularly branching, lateral black cilia and lobules present. Fungal hyphae thin, photobiont cells small globose, simple.

**Type genus:** *Daohugouthallus* Wang, Krings & Taylor<sup>15</sup>

**Type species:** *D. ciliiferus* Wang, Krings & Taylor<sup>15</sup>

Thallus foliose to subfruticose, about 5 cm high, 3 cm wide (Figures 4A and 4E); lobes slender, about 5 mm long and 0.5–1.5 mm wide, tips tapering, nearly dichotomous to irregular branching, with lateral rhizinate cilia, concolorous to thallus to black, 0.5–1.5 mm long (Figure 4B); black spots present in some areas; lobules present (Figure 4B); unknown disc-like structure superficial, or nearly terminal, 0.25–0.5 mm in diam., sometimes immersed (Figure 4C). Upper cortex conglutinate, c. 1  $\mu$ m thick (Figures 5A and 5B); photobiont cells globose, simple, mostly 1.5–2.5  $\mu$ m in diameter (Figures 5I, 5G, and 5C–5F), anastomosed by or adhered to the fungal hyphae with simple wall-to-wall interface; fungal hyphae filamentous, some shriveled, septate, mostly less than 1.25  $\mu$ m wide (Figures 4I–4K and 5A–5C).

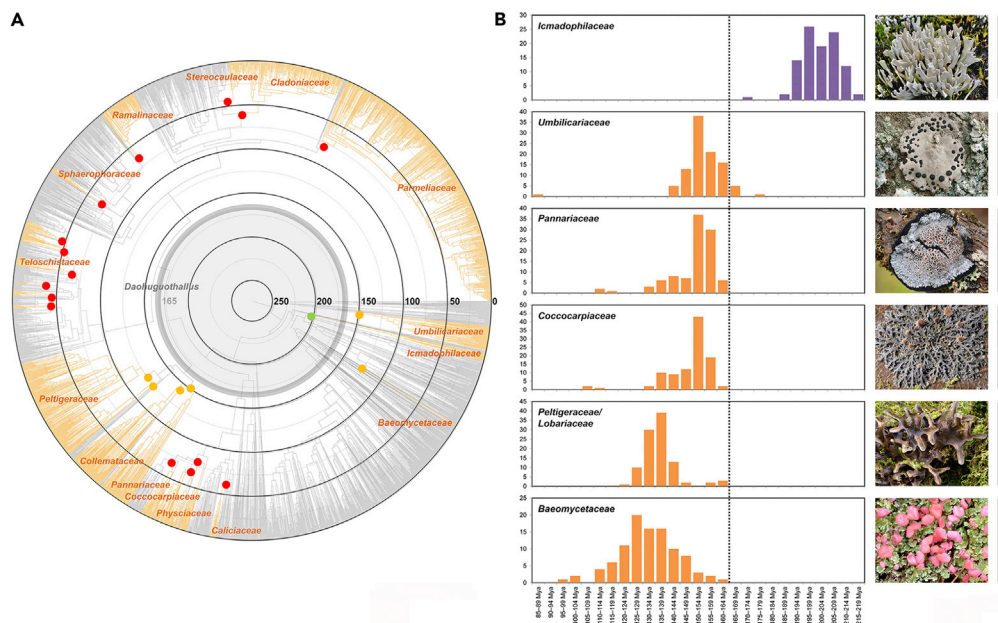


**Figure 3. Time-calibrated ML phylogeny of 3,373 Lecanoromycetes fungi and distribution of inferred divergence times for the oldest extant macrolichen families<sup>9</sup>**

(A) Macrolichen lineages are indicated in orange and the corresponding families are indicated. The age position of the *Daohugouthallus ciliiferus* fossil is marked by the bold gray circle. For details see Figure S2.

(B) The external morphology of selected representatives of each family is depicted to the right. The dotted line indicates the temporal placement of the *D. ciliiferus* fossil. The first three families, Peltigeraceae, and Collemataceae are likely asold or older than the fossil but do not fit morphologically and/or ecologically. The best morphological and ecological fit are Parmeliaceae, but that family is significantly younger.

**Substrate:** An unidentified gymnosperm branch (Figure 4D).

**Specimens examined:** China, Inner Mongolia, Ningcheng County, Shantou Township, near Daohugou Village, Daohugou 1, Jiulongshan Formation, Callovian–Oxfordian boundary interval, latest Middle Jurassic. CNU-LICHEN-NN2019001, CNU-LICHEN-NN2020001 (part and its counterpart), CNU-LICHEN-NN2020002, B0476P.

### Verification the epiphytic nature of *D. ciliiferus*

The new fossil material of *D. ciliiferus* grew on an unidentified gymnosperm branch (Figure 4A, 4D, and 4E), providing direct evidence to consider *D. ciliiferus* as the oldest known epiphytic lichen. However, the fossil material does not provide further details on how *D. ciliiferus* attached to the branch, because those very common connections that lichens attach to the substrate, such as rhizines, a lower tomentum, or an umbilicus, were not detected, and only the habitus reconstruction of the upper surface of *D. ciliiferus* in relation to its microhabitat was possible (Figure 6).

### DISCUSSION

GMA results provided a clue for clarifying the potential affinities of Daohugouthallaceae. The CVA plots based on the comparison with homologous landmarks of 66 extant macrolichens and two Parmeliaceae fossils showed Daohugouthallaceae being most similar to foliose Parmeliaceae, but in the light of the much older age of the fossil, this similarity cannot be interpreted as convincing evidence of a close relationship, also given the absence of diagnostic characters of the ascomata. Therefore, the introduction of a new and monogeneric family for this fossil seems justified in this case. Although we could not ascertain the higher classification of Daohugouthallaceae, it seems to be more distantly related to other extant macrolichens, such as Arthoniomycetes (fruticose thallus and *Trentepohlia*-type photobiont),<sup>30</sup> Lichinomycetes (saxicolous or terricolous habitat and cyanobacterial photobiont),<sup>31</sup> and Agaricomycetes (mushroom-like),<sup>32</sup> than to Lecanoromycetes. GMA is expected to be useful in the fossil and extant lichen taxonomy when traditional characters missed, especially after

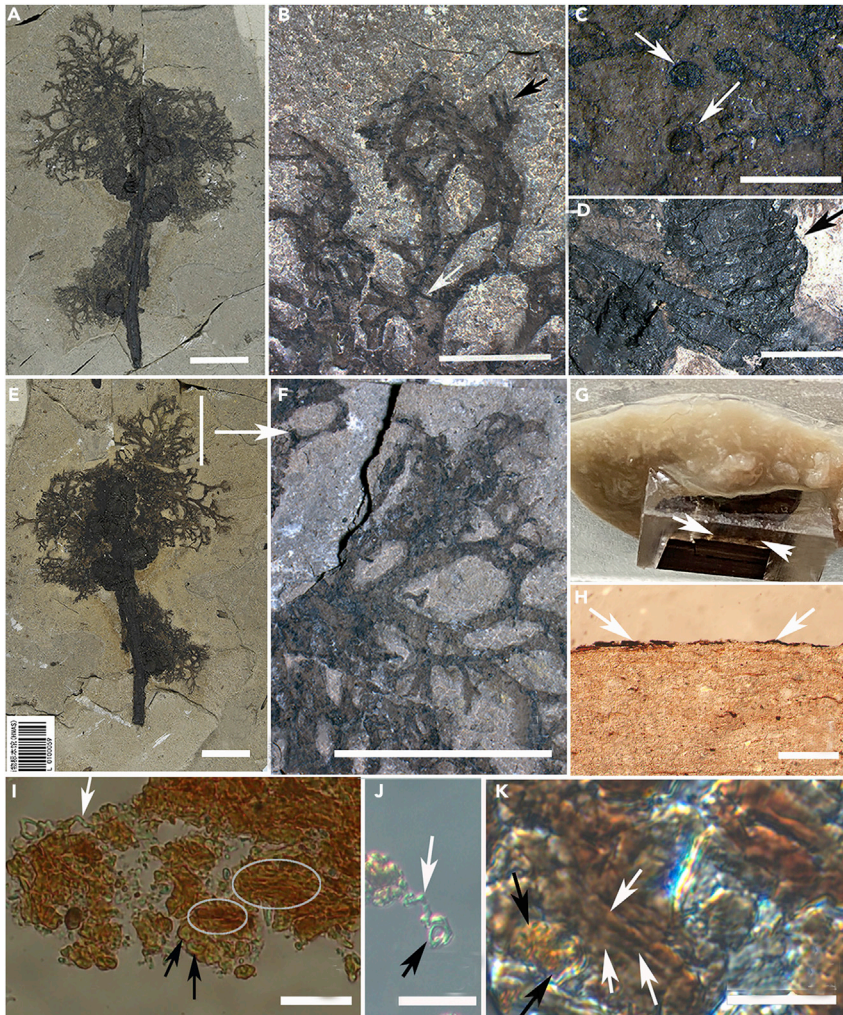


**Figure 4. Photos of fossil lichen *Daohugouthallus ciliiferus*, CNU-LICHEN-NN2020001**

- (A) External morphology of lichen thallus directly growing on the gymnosperm branch.  
 (B) Marginal rhizinate cilia and lobules marked by white and black arrows, respectively.  
 (C) Superficial and nearly immersed unknown disc-like structure.  
 (D) Gymnosperm branch with seed cones marked by black arrow.  
 (E) The counterpart of (a).  
 (F) Local zoom of the marked area of (E). Light microscopy of *D. ciliiferus*.  
 (G) Part of lobes in F with rock embedded in the light-cured resin for cross sectioning, the arrows indicating the location of lobes.  
 (H) Cross section of the fossil, the arrows indicating the dark areas corresponding to the lobes, about 10  $\mu\text{m}$  high, absence of thallus structure.  
 (I) Temporary slide of fossil fragments showed some photobiont cells, and conglutinated hyphae and single hypha, which are indicated by black arrows, white circles and white arrow, respectively.  
 (J) A single hypha (same to the one in photo i) and a possible hollow photobiont cell indicated by white and black arrow, respectively.  
 (K) Enlarged image of photobiont cells and conglutinated hyphae same to ones in photo I which are indicated by black and white circle and arrows, respectively. Scale bars: a, b, e, f = 1 cm; c = 5 mm; d = 1 mm; h = 100  $\mu\text{m}$ ; i, k = 10  $\mu\text{m}$ ; j = 20  $\mu\text{m}$ .

more detailed test based on more abundant extant lichen species, extracting those diagnostic characters but not including color and size and then transforming them into digital information.<sup>16</sup>

During the study, we noticed the photobiont cells were nearly half the size (1.5–2.5  $\mu\text{m}$  in diam.) and fungal hyphae were thinner (mostly less than 1.25  $\mu\text{m}$  wide) in *D. ciliiferus*, compared to extant macrolichens.

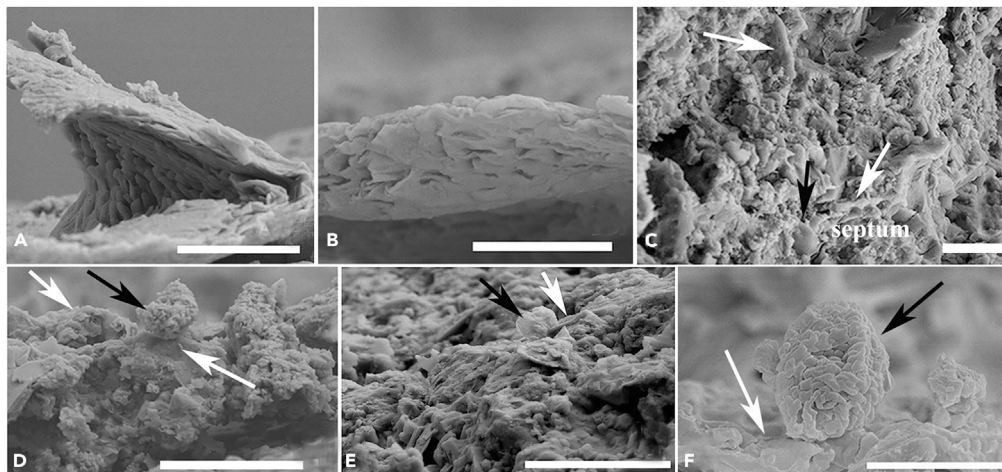


**Figure 5. Scanning electron microscopy (SEM) of *Daohugouthallus ciliiferus***

(A) Lichen upper cortex composed of conglomerated hyphal strand, CNU-LICHEN-NN2020001.  
(B) Morphology of upper cortex seen from lower side, conglomerated, stratiform and shriveled, CNU-LICHEN-NN2020001.  
(C) The hyphae with obvious septum observed in CNU-LICHEN-NN2020001, which is a diagnostic character of Ascomycota fungi.  
(D and E) Fungal and photobiont cell and their contact, CNU-LICHEN-NN2020001.  
(F) Fungal and photobiont cell and their contact, the photobiont cell is in framboidal form like, similar to the suspected green algae reported by Honegger et al. 2013 in some degree, CNU-LICHEN-NN2019001. Scale bars: The fungal hyphae and photobiont cells indicated by white and black arrows, respectively; a, c, d = 5  $\mu\text{m}$ ; b = 3  $\mu\text{m}$ ; e = 4  $\mu\text{m}$ ; f = 2  $\mu\text{m}$ .

Smaller photobiont (3–6  $\mu\text{m}$  in diam.)<sup>25</sup> and hyphae (1.1–3.5  $\mu\text{m}$  in diam.)<sup>11</sup> were also reported from other foliose macrolichen fossils, and Hartl et al.<sup>25</sup> considered the possible shrinkage to be related to the drying during fossilization. Previous studies have demonstrated that mycobiont and photobiont cultures isolated from a squamulose lichen survived up to eight and three months, respectively, under desiccation stress,<sup>33</sup> and the size of both algal and hyphal cells ultimately shrank by half. Thus, we hypothesize that foliose macrolichens like *D. ciliiferus* were more sensitive to drying or other environmental adversity, of which the photobiont and hyphae are more easily deformed. However, this hypothesis is partially contradicted by the finding that the fossil crustose lichens *C. devonicus* and *C. salopensis* (419–411 Mya)<sup>10</sup> had normally sized photobiont cells and hyphae. Certainly, it is also possible that the small size of the photobiont of *D. ciliiferus* is not an artifact, because in general, the size of extant green algae as photobiont is above 6  $\mu\text{m}$ ,<sup>11</sup> but there are some smaller coccoid green algae such as *Coccomyxa* (1.7–3.4  $\mu\text{m}$  in diam.).<sup>29</sup> *Coccomyxa* is known as the lichen photobiont of six extant lichenized orders, i.e., Baeomycetales, Lecanorales, Peltigerales, Pertusariales, Agaricales, and Cantharellales.<sup>34</sup> The first four belong to Lecanoromycetes (Ascomycota) and the latter two to Agaricomycetes (Basidiomycota). Therefore, a Jurassic alga like *Coccomyxa* in small size as photobiont of *D. ciliiferus* may be also conceivable.

The diversification of major macrolichen lineages after the Cretaceous–Paleogene (K–Pg) boundary was mainly concentrated within Lecanoromycetes.<sup>2,6,12</sup> Noticeably, the divergence time of Lecanoromycetes, was estimated at 300–250 Mya based on molecular clock analyses,<sup>7,9,23</sup> coinciding with the period after the end-Permian extinction. Considering the diverse Permian forests that were in existence around the world during that period,<sup>35</sup> this provided a potential ecological setting for the evolution of early epiphytic macrolichens; however, there are no fossils to support such an assumption. After the end-Triassic mass extinction 200 Mya, terrestrial vegetation and forest ecosystem recovered from Late Triassic onwards into the Early Jurassic.<sup>36</sup> This period could also have allowed the existence of epiphytic macrolichens, but again, no unambiguous fossil record exists that would support such a hypothesis, until our new specimen of Middle Jurassic *D. ciliiferus*, found attached to the branch of a gymnosperm fossil. Therefore, our material shows that gymnosperms, possibly representing a conifer, served as substrate for epiphytic macrolichens already in the Jurassic. The new material of *D. ciliiferus* thus fills the long gap between the beginning of the Permian and the end of the Cretaceous with regard to the demonstrable existence of epiphytic macrolichens. Even so, there still remains a large temporal gap of more than 100 My between this fossil and extant macrolichens that largely diversified in angiosperm-dominated forest ecosystem.<sup>6,8</sup>





**Figure 6. Habitus reconstruction of the fossil lichen *Daohugouthallus ciliiferus* growing on gymnosperm branches** (A) *D. ciliiferus* and its habitat; (B) Local enlarged drawing of *D. ciliiferus*. Drawing by Xiaoran Zuo.

Extant epiphytic macrolichens are crucial components of terrestrial woody ecosystems, including gymnosperm conifer forests,<sup>37</sup> playing an important role in the forest water and nutrient cycling.<sup>5</sup> Generally, epiphytic macrolichens attach to the bark or branch by lower surface, rhizines, tomentum, or an umbilicus. However, it remains unknown how *D. ciliiferus* attached to the gymnosperm branch. Epiphytic macrolichen diversity can be regarded as an indicator of forest ecosystems, as there is a significant correlation between epiphytic macrolichen diversity and tree species composition.<sup>5</sup> The fossil record and molecular clock studies indicate that gymnosperms diverged around 315 Mya,<sup>38</sup> whereas conifers originated approximately 300 Mya and diversified 190–160 Mya in the Early to Middle Jurassic<sup>39</sup> into the various families recognized today. Therefore, macrolichens may have played a role in Jurassic gymnosperm-dominated forest ecosystems comparable to extant macrolichens in present-day forests. The presence of an epiphytic macrolichen already in the Jurassic indicates that lichens and perhaps other epiphytes may already have contributed to the ecological complexity of paleo-forest ecosystems. Further exploration of potential Mesozoic lichen fossils is needed to shed more light on this issue.

### Limitations of the study

One limitation in our work is the sparse fossil record, with only one taxon of epiphytic macrolichen known so far from Mid-Jurassic, therefore, we cannot conclude it updated the time node of macrolichens diversification widely accepted around the K–Pg boundary (ca. 65 Mya). The other limitation is absence of some key diagnostic features in the *D. ciliiferus* fossil such as hamathecium, ascus, and ascospore structure, which limits the more accurate assessment on its phylogenetic position and further judgment on its relationship with the extant lichen lineages.

### STAR★METHODS

Detailed methods are provided in the online version of this paper and include the following:

- KEY RESOURCES TABLE
- RESOURCE AVAILABILITY
  - Lead contact
  - Materials availability
  - Data and code availability
- METHOD DETAILS
  - SEM and EDX examination
  - Geometric morphometric analysis
  - Molecular clock assessment

### SUPPLEMENTAL INFORMATION

Supplemental information can be found online at <https://doi.org/10.1016/j.isci.2022.105770>.

### ACKNOWLEDGMENTS

This work was supported by the National Natural Science Foundation of China [32070096 to X.W., 31970383 to Y.W., 42288201 and 32020103006 to D.R., 31922012 to H.L.], Ministry of Science and Technology of China [2019FY101808 to X.W.], National Key R & D Program of China (2022YFC2601200 to M.B.), the project of the

Northeast Asia Biodiversity Research Center (NABRI202203 to M.B.), and GDAS Special Project of Science and Technology Development [2022GDASZH-2022010106 to Y.W.]. The authors thank Mr. Yijie Tong for assisting in geometric morphometrics analysis, Dr. Chunli Li for assisting in taking SEM photos, Ms. Hong Deng and Ms. Haijuan Chen for lending and taking photos of lichen specimens in HMAS-L, Ms. Xiaoran Zuo for drawing the habitus reconstruction picture [Figure 6](#), Mr. Jujie Guo for cutting the fossil, Ms. Shukang Zhang for making fossil thin slices, and Mr. Xun Jin for EDX examination.

## AUTHOR CONTRIBUTIONS

Q.X.Y.: Literatures investigation, geometric morphometric analysis, molecular data collection and analysis, original draft editing; Y.Y.W.: SEM photos taking and analysis, molecular data analysis, original draft editing; R.L.: Conceptualization, molecular clock analysis, validation, draft review and editing; T.L.: Conceptualization, validation, draft review and editing; ZYD: molecular analysis, draft review and editing; Y.K.C.: Geometric morphometric analysis, draft review and editing; M.B.: Geometric morphometric analysis, draft review and editing; D.R.: Conceptualization, resources collection, supervision, project administration, validation, funding acquisition, draft review and editing; J.C.W.: Conceptualization, supervision, validation, draft review and editing; H.L.: Conceptualization, molecular analysis, validation, draft review and editing; Y.J.W.: Conceptualization, resources collection, supervision, funding acquisition, validation, draft review and editing; X.L.W.: Conceptualization, supervision, geometric morphometric analysis, SEM photos taking and analysis, data curation, funding acquisition, project administration, validation, original draft writing, review and editing.

## DECLARATION OF INTERESTS

We declare we have no competing interests.

Received: May 21, 2022

Revised: November 3, 2022

Accepted: December 6, 2022

Published: January 20, 2023

## REFERENCES

- Hawksworth, D.L., and Grube, M. (2020). Lichens redefined as complex ecosystems. *New Phytol.* 227, 1281–1283. <https://doi.org/10.1111/nph.16630>.
- Lücking, R., and Nelsen, M.P. (2018). Ediacarans, protolichens, and lichen-derived *Penicillium*: a critical reassessment of the evolution of lichenization in fungi. In *Transformative paleobotany*, M. Krings, C.J. Harper, and N.R. Cúneo, et al., eds. (Academic Press), pp. 551–590. <https://doi.org/10.1016/B978-0-12-813012-4.00023-1>.
- Lumbsch, H.T., and Rikkinen, J. (2017). Evolution of lichens. In *The fungal community: its organization and role in the ecosystem*, J. Dighton, J. White, and F.L. Boca Raton, eds. (CRC Press), pp. 53–62. <https://doi.org/10.1201/9781315119496-5>.
- Nash, T.H., III (2008). *Lichen Biology*, 2nd edition (Cambridge University Press).
- Klein, J., Low, M., Thor, G., Sjögren, J., Lindberg, E., and Eggers, S. (2021). Tree species identity and composition shape the epiphytic lichen community of structurally simple boreal forests over vast areas. *PLoS One* 16, e0257564. <https://doi.org/10.1371/journal.pone.0257564>.
- Huang, J.P., Kraichak, E., Leavitt, S.D., Nelsen, M.P., and Lumbsch, H.T. (2019). Accelerated diversifications in three diverse families of morphologically complex lichen-forming fungi link to major historical events. *Sci. Rep.* 9, 8518. <https://doi.org/10.1111/nph.12000>.
- Kraichak, E., Huang, J.P., Nelsen, M., Leavitt, S.D., and Lumbsch, H.T. (2018). A revised classification of orders and families in the two major subclasses of Lecanoromycetes (Ascomycota) based on a temporal approach. *Bot. J. Linn. Soc.* 188, 233–249. <https://doi.org/10.1093/botlinnean/boy060>.
- Lücking, R., Hodkinson, B.P., and Leavitt, S.D. (2017). The 2016 classification of lichenized fungi in the Ascomycota and Basidiomycota – approaching one thousand genera. *Bryologist* 119, 361–416. <https://doi.org/10.1639/0007-2745-119.4.361>.
- Nelsen, M.P., Lücking, R., Boyce, C.K., Lumbsch, H.T., and Ree, R.H. (2020). The macroevolutionary dynamics of symbiotic and phenotypic diversification in lichens. *Proc. Natl. Acad. Sci. USA* 117, 21495–21503. <https://doi.org/10.1073/pnas.2001913117>.
- Honegger, R., Edwards, D., and Axe, L. (2013). The earliest records of internally stratified cyanobacterial and algal lichens from the lower Devonian of the Welsh Borderland. *New Phytol.* 197, 264–275. <https://doi.org/10.1111/nph.12000>.
- Matsunaga, K.K.S., Stockey, R.A., and Tomescu, A.M.F. (2013). *Honeggeriella complexa* gen. et sp. nov., a heteromerous lichen from the lower cretaceous of Vancouver Island (British Columbia, Canada). *Am. J. Bot.* 100, 450–459. <https://doi.org/10.3732/ajb.1200470>.
- Kaasalainen, U., Schmidt, A.R., and Rikkinen, J. (2017). Diversity and ecological adaptations in Palaeogene lichens. *Nat. Plants* 3, 17049. <https://doi.org/10.1038/nplants.2017.49>.
- Fang, H., Labandeira, C.C., Ma, Y., Zheng, B., Ren, D., Wei, X., Liu, J., and Wang, Y. (2020). Lichen mimesis in mid-Mesozoic lacewings. *Elife* 9, e59007. <https://doi.org/10.7554/eLife.59007>.
- Gargas, A., DePriest, P.T., Grube, M., and Tehler, A. (1995). Multiple origins of lichen symbioses in fungi suggested by SSU rDNA phylogeny. *Science* 268, 1492–1495. <https://doi.org/10.1126/science.7770775>.
- Wang, X., Krings, M., and Taylor, T.N. (2010). A thalloid organism with possible lichen affinity from the Jurassic of northeastern China. *Rev. Palaeobot. Palynol.* 162, 591–598. <https://doi.org/10.1016/j.revpalbo.2010.07.005>.
- James Rohlf, F., and Marcus, L.F. (1993). A revolution in morphometrics. *Trends Ecol.*

- Evol. 8, 129–132. [https://doi.org/10.1016/0169-5347\(93\)90024-J](https://doi.org/10.1016/0169-5347(93)90024-J).
17. Bookstein, F.L. (1991). Thin-plate splines and the atlas problem for biomedical images. In *Information Processing in Medical Imaging*, A.C.F. Colchester and D.J. Hawkes, eds. (Springer), pp. 326–342.
  18. Bai, M. (2017). Geometric morphometrics: current and future in China. *Zool. Syst.* 42, 1–3. <https://doi.org/10.1186/zs.201701>.
  19. Cheng, L., Tong, Y., Zhao, Y., Sun, Z., Wang, X., Ma, F., and Bai, M. (2022). Study on the relationship between richness and morphological diversity of higher taxa in the darkling beetles (Coleoptera: Tenebrionidae). *Diversity* 14, 60. <https://doi.org/10.3390/d14010060>.
  20. Lu, Y., Ballerio, A., Wang, S., Zou, Z., Gorb, S.N., Wang, T., Li, L., Ji, S., Zhao, Z., Li, S., et al. (2022). The evolution of conglobation in Ceratocanthinae. *Commun. Biol.* 5, 777. <https://doi.org/10.1038/s42003-022-03685-2>.
  21. Tong, Y.J., Yang, H.D., Jenkins Shaw, J., Yang, X.K., and Bai, M. (2021). The relationship between genus/species richness and morphological diversity among subfamilies of jewel beetles. *Insects* 12, 24. <https://doi.org/10.3390/insects12010024>.
  22. Xu, H., Kubán, V., Volkovitch, M.G., Ge, S., Bai, M., and Yang, X. (2013). Morphological variability and taxonomy of *Coraebus hastanus* gory & Laporte de Castelnau, 1839 (Coleoptera: Buprestidae: agrilinae: Coraebini: Coraebina). *Zootaxa* 3682, 178–190. <https://doi.org/10.11646/zootaxa.3682.1.9>.
  23. Lutzoni, F., Nowak, M.D., Alfaro, M.E., Reeb, V., Miadlikowska, J., Krug, M., Arnold, A.E., Lewis, L.A., Swofford, D.L., Hibbett, D., et al. (2018). Contemporaneous radiations of fungi and plants linked to symbiosis. *Nat. Commun.* 9, 5451. <https://doi.org/10.1038/s41467-018-07849-9>.
  24. Colpan, C.O., Nalbant, Y., and Ercelik, M. (2018). Fundamentals of fuel cell technologies. In *Comprehensive Energy Systems*, vol. 4, I. Dincer, ed. (Elsevier), pp. 1107–1130. <https://doi.org/10.1016/b978-0-12-809597-3.00446-6>.
  25. Hartl, C., Schmidt, A.R., Heinrichs, J., Seyfullah, L.J., Schäfer, N., Gröhn, C., Rikkinen, J., and Kaasalainen, U. (2015). Lichen preservation in amber: morphology, ultrastructure, chemofossils, and taphonomic alteration. *Foss. Rec.* 18, 127–135. <https://doi.org/10.5194/fr-18-127-2015>.
  26. Rambold, G., Triebel, D., and Hertel, H. (1993). *Imadophilaceae, a new family in the Leotiales*. *Bibl. Lichenol.* 53, 217–240.
  27. Ezhkin, A.K., and Ohmura, Y. (2021). Notes to Pannariaceae species in taiwan. *Taiwania* 66, 575–579. <https://doi.org/10.6165/tai.2021.66.575>.
  28. Wei, J.C., and Jiang, Y.M. (1993). *The Asian Umbilicariaceae (Ascomycota) (International Academic Publishers)*.
  29. Wu, J.N., and Liu, H.J. (2012). *Flora Lichenum Sinicorum. In Peltigerales (I), 1 Peltigerales (I) (Science Press)*.
  30. Tehler, A. (2011). *Roccella, the Sonoran species reviewed. Bibl. Lichenol.* 106, 309–318.
  31. Prieto, M., Westberg, M., and Schultz, M. (2015). New records of Lichinomycetes in Sweden and the Nordic countries. *Herzogia* 28, 142–152. <https://doi.org/10.13158/hea.28.1.2015.142>.
  32. Nelsen, M.P. (2021). Sharing and double-dating in the lichen world. *Mol. Ecol.* 30, 1751–1754. <https://doi.org/10.1111/mec.15884>.
  33. Zhang, T., and Wei, J. (2011). Survival analyses of symbionts isolated from *Endocarpon pusillum* Hedwig to desiccation and starvation stress. *Sci. China Life Sci.* 54, 480–489. <https://doi.org/10.1007/s11427-011-4164-z>.
  34. Cao, S., Zhang, F., Zheng, H., Peng, F., Liu, C., and Zhou, Q. (2018). *Coccomyxa greatwallensis* sp. nov. (Trebouxiophyceae, Chlorophyta), a lichen epiphytic alga from Fildes Peninsula, Antarctica. *PhytoKeys* 110, 39–50. <https://doi.org/10.3897/phytokeys.110.26961>.
  35. Wang, J., Pfefferkorn, H.W., Zhang, Y., and Feng, Z. (2012). Permian vegetational Pompeii from Inner Mongolia and its implications for landscape paleoecology and paleobiogeography of Cathaysia. *Proc. Natl. Acad. Sci. USA* 109, 4927–4932. <https://doi.org/10.1073/pnas.1115076109>.
  36. Bonis, N.R., and Kürschner, W.M. (2012). Vegetation history, diversity patterns, and climate change across the Triassic/Jurassic boundary. *Paleobiology* 38, 240–264. <https://doi.org/10.1666/09071.1>.
  37. Wei, X.L., Leavitt, S.D., Huang, J.P., Esslinger, T.L., Wang, L.S., Moncada, B., Lücking, R., Divakar, P.K., and Lumbsch, H.T. (2017). Parallel Miocene-dominated diversification of the lichen-forming fungal genus *Oropogon* (Parmeliaceae, Ascomycota) in different continents. *Taxon* 66, 1269–1281. <https://doi.org/10.12705/666.1>.
  38. Nie, Y., Foster, C.S.P., Zhu, T., Yao, R., Duchêne, D.A., Ho, S.Y.W., and Zhong, B. (2020). Accounting for uncertainty in the evolutionary timescale of green plants through clock-partitioning and fossil calibration strategies. *Syst. Biol.* 69, 1–16. <https://doi.org/10.1093/sysbio/sy032>.
  39. Leslie, A.B., Beaulieu, J., Holman, G., Campbell, C.S., Mei, W., Raubeson, L.R., and Mathews, S. (2018). An overview of extant conifer evolution from the perspective of the fossil record. *Am. J. Bot.* 105, 1531–1544. <https://doi.org/10.1002/ajb2.1143>.
  40. Rohlf, F.J. (2006). *tpsDig, Digitize Landmarks and Outlines, Version 2.05 (Stony Brook)*.
  41. Klingenberg, C.P. (2011). Computer program note MorphoJ: an integrated software package for geometric morphometrics. *Mol. Ecol. Resour.* 11, 353–357. <https://doi.org/10.1111/j.1755-0998.2010.02924.x>.
  42. Rambaut, A. (2018). *FigTree, a Graphical Viewer of Phylogenetic Trees (Version v1.4.4)*.
  43. Smith, S.A., and O’Meara, B.C. (2012). treePL: divergence time estimation using penalized likelihood for large phylogenies. *Bioinformatics* 28, 2689–2690. <https://doi.org/10.1093/bioinformatics/bts492>.
  44. He, H.Y., Wang, X.L., Zhou, Z.H., Zhu, R.X., Jin, F., Wang, F., Ding, X., and Boven, A. (2004). <sup>40</sup>Ar/<sup>39</sup>Ar dating of ignimbrite from Inner Mongolia, northeastern China, indicates a post-Middle Jurassic age for the overlying Daohugou Bed. *Geophys. Res. Lett.* 31, L20609. <https://doi.org/10.1029/2004GL020792>.
  45. Liu, Y., Liu, Y., Ji, S., and Yang, Z. (2006). U–Pb zircon age for the Daohugou Biota at Ningcheng of Inner Mongolia and comments on related issues. *Chin. Sci. Bull.* 51, 2634–2644. <https://doi.org/10.1007/s11434-006-2165-2>.

## STAR★METHODS

## KEY RESOURCES TABLE

| REAGENT or RESOURCE                     | SOURCE                        | IDENTIFIER  |
|---|-------------------------------|---|
| <b>Biological samples</b>               |                               |   |
| Fossil specimen of <i>D. ciliiferus</i> | CNU                           | CNU-LICHEN-NN2019001  |
| Fossil specimen of <i>D. ciliiferus</i> | CNU                           | CNU-LICHEN-NN2020001  |
| Fossil specimen of <i>D. ciliiferus</i> | CNU                           | CNU-LICHEN-NN2020002  |
| Fossil specimen of <i>D. ciliiferus</i> | CNU                           | B0476P  |
| <i>Hypotrachyna cirrhata</i>            | HMAS                          | HMAS-L 8322   |
| <i>Peltigera praetextata</i>            | HMAS                          | HMAS-L 13030  |
| <b>Software and algorithms</b>          |                               |   |
| TPS-DIG 2.05                            | Rohlf <sup>40</sup>           | <a href="https://tpsdig2.software.informer.com/">https://tpsdig2.software.informer.com/</a>           |
| MORPHO J 1.06a                          | Klingenberg <sup>41</sup>     | <a href="http://www.flywings.org.uk/MorphoJ_PAGE.htm">http://www.flywings.org.uk/MorphoJ_PAGE.htm</a> |
| FigTree 1.4.4                           | Rambaut <sup>42</sup>         | <a href="http://tree.bio.ed.ac.uk/software/figtree/">http://tree.bio.ed.ac.uk/software/figtree/</a>   |
| treePL v1.044                           | Smith & O'Meara <sup>43</sup> | <a href="https://github.com/blackrim/treePL">https://github.com/blackrim/treePL</a>                   |
| <b>Other</b>                            |                               |   |
| Stereomicroscope                        | Olympus                       | SZX7  |
| Digital camera system                   | Mshot                         | MD50  |
| One-component resin                     | EXAKT                         | Technovit 7200  |
| Cutting system                          | EXAKT                         | 300CP   |
| Variable speed grinding system          | EXAKT                         | 400CS   |
| Ion Sputter coater                      | HITACHI                       | E-1045  |
| Scanning electron microscope            | HITACHI                       | SU8010  |
| Scanning electron microscope            | Zeiss                         | MA EVO25  |
| Energy Dispersive X-ray Spectroscopy    | Oxford                        | X-act (8–10 mm)   |

## RESOURCE AVAILABILITY

## Lead contact

Further information and requests for resources and reagents should be directed to and will be fulfilled by the Lead Contact, Xinli Wei ([weixl@im.ac.cn](mailto:weixl@im.ac.cn))

## Materials availability

Fossil specimens of *D. ciliiferus* (CNU-LICHEN-NN2019001, CNU-LICHEN-NN2020001 (part and its counterpart), CNU-LICHEN-NN2020002, B0476P) were collected from the Daohugou locality of the Jiulongshan Formation, near Daohugou Village, Ningcheng County, approximately 80 km south of Chifeng City, in the Inner Mongolia Autonomous Region, China (119°14.318'E, 41°18.979'N) and are deposited in the Key Lab of Insect Evolution and Environmental Changes, College of Life Sciences and Academy for Multidisciplinary Studies, Capital Normal University (CNU), in Beijing, China. The age of this formation is 168–152 Ma based on <sup>40</sup>Ar/<sup>39</sup>Ar and <sup>206</sup>Pb/<sup>238</sup>U isotopic analyses.<sup>44,45</sup> The lichen specimens *Hypotrachyna cirrhata* (HMAS-L 8322) and *Peltigera praetextata* (HMAS-L 13030) are deposited in the Fungarium (HMAS), Institute of Microbiology, Chinese Academy of Sciences, in Beijing, China.

## Data and code availability

All data reported in this paper will be shared by the [lead contact](#) upon request.

This study did not generate original code.

Any additional information required to reanalyze the data reported in this work is available from the [lead contact](#) upon reasonable request.

## METHOD DETAILS

### SEM and EDX examination

The lichen fossils were examined and photographed using an Olympus SZX7 Stereomicroscope attached to a Mshot MD50 digital camera system. For selected fossil we made cross sections using a stonecutter, one piece was embedded in EXAKT Technovit 7200 one-component resin, then cut using an EXAKT 300CP cutting system. The thin sections were ground and polished to the thickness of about 20  $\mu\text{m}$  using an EXAKT 400CS variable speed grinding system with P500 and P4000 abrasive papers; one piece of the fossil together with two pieces of extant lichen species *H. cirrhata* (lichen 1 = extant chlorolichen HMAS-L 8322) and *P. praetextata* (lichen 2 = extant cyanolichen HMAS-L 13030) were sputter-coated with gold particles using Ion Sputter E-1045 (HITACHI). SEM images were recorded using a scanning electron microscope (Hitachi SU8010); the above-mentioned pieces of fossil and two extant lichens were analyzed with a Zeiss MA EVO25 scanning electron microscope under a high vacuum mode by using an accelerating voltage of 20 kV. Energy Dispersive X-ray Spectroscopy (EDX/EDS) spectra were obtained with an Oxford X-act detector. The working distance was kept between 8 and 10 mm. Acquisition time was set up to 60 s for each EDS spectrum. Plates were composed in Adobe Photoshop. Most lab work was performed at the Institute of Microbiology, except the stonecutter was operated at the Institute of Geology and Geophysics, and the fossil thin sectioning and EDX were taken at the Institute of Vertebrate Paleontology and Paleoanthropology. All the above three Institutes are in Beijing and subordinate to Chinese Academy of Sciences.

### Geometric morphometric analysis

For geometric morphometrics, 149 images (Figure S1) of 66 representative extant macrolichen species were selected from 15 families and 9 orders in both Ascomycota and Basidiomycota (Table S3), including specimens deposited in HMAS-L, photos provided by Robert Lücking, and pictures downloaded from the CNALH (Consortium of North American Herbaria) Image Library <https://lichenportal.org/cnalh/imagelib/> and the *Hypogymnia* Media Gallery <http://hypogymnia.myspecies.info/gallery>, together with accepted Parmeliaceae fossils,<sup>12</sup> and *D. ciliiferus* fossil, among which 14 species had more than 2 samples and images, 15 species had only one sample each but more than 2 images, and 37 species had one image each, together with two images of accepted Parmeliaceae fossils, and 25 sub-images cut from the images of *D. ciliiferus* fossil. The sampling number of images in this study comprehensively considered the quality requirement for the geometric morphometric analysis, representativeness and availability of the discernable topology of thallus lobes or branches. The whole image set was divided into five groups according to lobes types: microfoliose group, the *D. ciliiferus* fossil group, a long branches group, a wide-lobed group, and a fruticose group (Table S4). The selected images were two-dimensional graphs with two views of the front or back of the thallus where the branch tips were clearly recognizable. To orient the images in the same direction, they were adjusted so that the end of the branches faced right. Images were named in a unified format: growth type-order-family-genus-species (sample number) except for the two selected reference fossil images only corresponding to family name.

The external forms were represented by one curve extracted from the end of branches or lobes and the curve was resampled into 60 semi-landmarks by length (Figure S3). The starting point of the curve was selected as a point on the upper edge of the lobe or branch near the center or substrate, and after describing the outline of the whole lobe or branch, the endpoint returning to the lower edge near the starting point. The curves and semi-landmarks were digitized using TPS-DIG 2.05.<sup>40</sup> To merge all semi-landmarks into the same data file to produce the dataset for morphological analysis, the data file was opened as text file to convert the semi-landmarks to landmarks, by deleting the line with the curve number and point number and replacing the landmark number by the point number.<sup>21</sup> MORPHO J 1.06a<sup>41</sup> was used for subsequent analysis of the dataset. Through Procrustes analysis, the morphological data of all test features were placed in the same dimensional vector space to screen out physical factors such as size. Principal component analysis (PCA) and geometric modeling of the mathematical space formed by PC axis were used to coordinate the shape changes of the entire dataset. We then selected the dataset to generate a covariance matrix. In this context, the first two principal components corresponding to the highest cumulative variance represent the best variation pattern of test shape. The

relationships among different morphological groups were then visualized through canonical variate analysis (CVA).

### **Molecular clock assessment**

The time-calibrated maximum likelihood phylogeny of 3,373 Lecanoromycetes fungi was taken from the supplementary data provided by Nelsen et al.<sup>9</sup> It was edited for content and style using FigTree 1.4.4,<sup>42</sup> highlighting the clades including macrolichens. According to Nelsen et al.,<sup>9</sup> the time-calibrated tree was originally constructed from a partitioned ML analysis using penalized likelihood in treePL v. 1.044.<sup>43</sup>